Prolonged Physiological Entrapment of Glutamate in the Synaptic Cleft of Cerebellar Unipolar Brush Cells

GREGORY A. KINNEY, LINDA S. OVERSTREET, AND N. TRAVERSE SLATER
Department of Physiology, Northwestern University Medical School, Chicago, Illinois 60611

Kinney, Gregory A., Linda S. Overstreet, and N. Traverse Slater. Prolonged physiological entrapment of glutamate in the synaptic cleft of cerebellar unipolar brush cells. *J. Neurophysiol.* 78: 1320–1333, 1997. The cellular mechanism underlying the genesis of the long-lasting α-amino-3-hydroxy-5-methyl-4-isoxazolepropionic acid (AMPA)-receptor-mediated excitatory postsynaptic currents (EPSCs) at the mossy fiber (MF)–unipolar brush cell (UBC) synapse in rat vestibular cerebellum was examined with the use of whole cell and excised patch-clamp recording methods in thin cerebellar slices. Activation of MFs evokes an all-or-none biphasic AMPA-receptor-mediated synaptic current with a late component that peaks at 100–800 ms, which has been proposed to originate from an entrapment of glutamate in the MF-UBC synaptic cleft and is generated by the steady-state activation of AMPA receptors. Bath application of cyclothiazide, which blocks desensitization of AMPA receptors, produced a dose-dependent enhancement of the amplitude of the synaptic current (median effective dose 30 μM) and slowing of the rise time of the fast EPSC. *N*-methyl-D-aspartate-receptor-mediated EPSCs in UBCs were not potentiated in amplitude or time course by cyclothiazide (100 μM). The dose-response relations for the steady-state current evoked by glutamate acting at AMPA receptors in excised outside-out patches from UBC and granule somatic membranes was biphasic, peaking at 50 μM and declining to 50–70% of this value at 1 mM glutamate. When glutamate was slowly washed from patches to simulate the gradual decline of glutamate in the synapse, a late hump in the transmembrane current was observed in patches from both cell types. The delivery of a second MF stimulus at the peak of the slow EPSC evoked a fast EPSC of reduced amplitude followed by an undershoot of the subsequent slow current, consistent with the hypothesis that the peak of the slow EPSC reflects the peak of the biphasic steady-state dose-response curve. Estimates of receptor occupancy and glutamate concentration derived from the ratio of fast EPSC amplitudes, and the amplitude and polarity of the initial steady-state current in paired-pulse experiments, predict a slow decline of glutamate with a time constant of 800 ms, declining to ineffective concentrations at 5.4 s. Manipulation of cleft glutamate concentration by lowered extracellular calcium or delivery of brief stimulus trains abolished the slow EPSC and restored the undershoot to paired stimuli, respectively, in a manner consistent with a prolonged lifetime of glutamate in the cleft. The slow component of the EPSC was prolonged in duration by the glutamate reuptake inhibitor L-*trans*-pyrrolidine-2,4-dicarboxylate, suggesting that glutamate transport contributes to the time course of the synaptic current in UBCs. The data support the notion that the MF-UBC synapse represents an ultrastructural specialization to effectively entrap glutamate for unusually prolonged periods of time following release from MF terminals. The properties of the postsynaptic receptors and constraints on diffusional escape of glutamate imposed by synaptic ultrastructure and glutamate transporters act in concert to sculpt the time course of the resulting slow EPSC. This in turn drives a long-lasting train of action potentials in response to single presynaptic stimuli.

INTRODUCTION

Glutamate is the principal excitatory neurotransmitter in the vertebrate CNS, and the factors that govern the time course of excitatory postsynaptic currents (EPSCs) at glutamatergic synapses is a topic of considerable importance in understanding information processing within the brain (Collingridge and Lester 1990; Mayer and Westbrook 1987; Storm-Mathisen et al. 1995). The time course of glutamatergic EPSCs is governed by many factors, which include the identity and molecular composition of postsynaptic receptors, the ultrastructural geometry of the synaptic cleft, proximity of coactive synapses, synchrony of presynaptic release, and localization of glutamate transporters (Clements 1996; Edmonds et al. 1995; Isaacson and Walmsley 1995; Jonas and Spruston 1994; Jones and Westbrook 1996; McBain and Mayer 1994; Nakanishi 1992; Takahashi et al. 1997). At the majority of glutamatergic synapses the EPSC is composed of both fast α-amino-3-hydroxy-5-methyl-4-isoxazolepropionic acid (AMPA) and slower *N*-methyl-D-aspartate (NMDA)-receptor-mediated components. The time course of the AMPA-receptor-mediated component of the synaptic current is generally very brief, reflecting the short lifetime of glutamate in the synaptic cleft (1–2 ms), because most glutamatergic synapses are of small diameter and glutamate is removed rapidly from the vicinity of postsynaptic receptors congregated at the postsynaptic density by diffusion. AMPA receptors desensitize very rapidly on exposure to glutamate (Tang et al. 1989; Trussell and Fischbach 1989) and are of low affinity (Patneau and Mayer 1990). Consequently the decay of the EPSC can be shaped both by receptor desensitization and the subsequent dissociation of glutamate from the receptor (Clements 1996; Edmonds et al. 1995; Jonas and Spruston 1994; Jones and Westbrook 1996).

A notable exception to these principles has recently emerged with the discovery of a new class of neurons in the cerebellum, the unipolar brush cells (UBCs) (Mugnaini et al. 1997; Slater et al. 1997a,b). UBCs are small neurons located in the granular layer of vestibular regions of the mammalian cerebellum (Altman and Bayer 1977; Floris et al. 1994; Mugnaini and Floris 1994) receiving synaptic input from a single mossy fiber (MF) that interdigitates with the entire dendritic brush, forming a giant synapse with a very

extensive area of synaptic apposition (12–40 μm^2) (Mugnaini et al. 1994). The MF-UBC synapse is unusual in that multiple release sites are apposed to a continuous postsynaptic density within which postsynaptic ionotropic glutamate receptors are localized (Jaarsma et al. 1995; Mugnaini et al. 1994; Rossi et al. 1995). Thus, after release from the presynaptic terminal, glutamate molecules cannot rapidly escape from the cleft by diffusion into extracellular space, precluding the rapid termination of the EPSC. The EPSC at most MF-UBC synapses is glutamatergic, with both AMPA- and NMDA-receptor-mediated components. It is unusual in that both components are very prolonged in duration, giving rise to an excitatory postsynaptic potential (EPSP) lasting many seconds with an associated burst of action potentials (Rossi et al. 1995; Slater et al. 1997b). The AMPA-receptor-mediated EPSC at this synapse is particularly unusual in that it is biphasic, with a rapidly activating and decaying component that is followed by a slow EPSC (time-to-peak ~300 ms) (Rossi et al. 1995).

It has been proposed that the ultrastructure of the MF-UBC synapse represents a specialization to entrap glutamate within the cleft for prolonged periods following release and that the biphasic nature of the AMPA component of the EPSC reflects an interplay between the slowly decaying concentration of glutamate ([glu]) and the dose dependence of the steady-state AMPA-receptor-mediated current (Rossi et al. 1995). Because the lifetime of glutamate at conventional synapses is very brief, such steady-state currents are not normally observed. The dose-response relation for the steady-state AMPA-receptor-mediated current in other cell types is biphasic (Geoffroy et al. 1991; Raman and Trussell 1992). At the MF-UBC synapse it was proposed that the biphasic AMPA-receptor-mediated synaptic current reflects this property (Rossi et al. 1995) in the following manner. After release, a fast EPSC will be observed reflecting activation of AMPA receptors that decays rapidly to a steady-state level because of desensitization and equilibration by diffusion within the cleft volume. The [glu] within the cleft will then further decay as the transmitter slowly escapes by diffusion into extracellular space. A slow EPSC will be observed as the cleft [glu] declines across the peak of the biphasic dose-response relations for the steady-state current. This ''glutamate entrapment hypothesis'' proposed by Rossi et al. (1995) is further studied here with the use of a combination of whole cell and excised patch recording methods to critically evaluate the hypothesis. The results provide strong support for the notion that the MF-UBC synapse is indeed highly specialized for the entrapment of transmitter within the cleft.

Preliminary reports of some of these data have been presented (Kinney et al. 1995, 1996; Slater and Kinney 1996).

METHODS

Preparation of brain slices

The methods for the preparation of thin brain slices and patch-clamp recording of visually identified UBCs and granule cells in thin cerebellar slices employed were similar to those previously described (D'Angelo et al. 1993; Ebralidze et al. 1996; Rossi et al. 1995; Silver et al. 1992). Experiments were conducted on Sprague-Dawley rats of either sex, ages 8–30 days postnatal. Animals were anesthetized with the use of isoflurane by inhalation and killed by decapitation with the use of a guillotine while under general anesthesia. The brain was removed by dissection and placed in a chilled (0–5°C) extracellular solution of the following composition (in mM): 126 NaCl, 3 KCl, 2.5 $CaCl_2$, 1.3 $MgSO_4$, 1.25 NaH_2PO_4, 26 $NaHCO_3$, and 10 D-glucose, gassed with 95% O_2-5% CO_2, pH 7.4, osmolarity 310 mosmol. Thin (150 μm thick) parasagittal slices of cerebellar vermis were cut with the use of a vibrating tissue chopper (Vibratome). Slices were maintained at room temperature after the initial hour of incubation until needed for recording.

For recording, slices were transferred to a submersion chamber mounted on the stage of an upright microscope (Leitz Laborlux) and viewed with a Zeiss ×40 (0.75 numerical aperture) water-immersion objective with Hoffman Contrast Optics. The slices were continuously perfused throughout the experiment with external medium at room temperature (20–22°C). All recordings were made from UBCs and granule cells in the granular layer of the nodulus and uvula. UBCs were identified in living slices by their larger soma diameter and greater whole cell capacitance than adjacent granule cells and by their prolonged synaptic response to white matter stimulation.

Patch-clamp recording and synaptic stimulation

Patch recording pipettes were fabricated from thick-walled borosilicate glass capillaries (DC resistance 3–10 MΩ when filled with internal solution) with the use of a Flaming-Brown horizontal pipette puller (Sutter Instruments). In the majority of experiments electrodes were filled with an internal solution containing (in mM): 145 cesium methanesulphonate, 10 QX-314, 2 $MgCl_2$, 5 K_2ATP, 0.5 ethylene glycol-bis(β-aminoethyl ether)-*N,N,N′,N′*-tetraacetic acid, and 5 *N*-2-hydroxyethylpiperazine-*N′*-2-ethanesulfonic acid, pH 7.2, osmolarity adjusted to 280 mosmol. Patch pipettes were mounted in the headstage input of a stage-mounted micromanipulator and positioned over the soma of the neuron by visual control. Transmembrane voltage and current were recorded with the use of an Axopatch 1D or 200A amplifier (filtered at 10 kHz, −3 dB), stored on video tape (VR-10C, Instrutec), and played back off-line for analysis with the use of pClamp (version 0.6.0.1) software (Axon Instruments) running on a PC-compatible 486 microcomputer (Dell). Conventional methods for whole cell recording and the preparation of excised (Edwards et al. 1989; Hamill et al. 1981) or nucleated outside-out membrane patches (Sather et al. 1992) were employed. The reference electrode was connected to the bath by means of a KCl-agar bridge. All experiments were conducted at a holding potential of −80 mV unless otherwise noted.

Concentric bipolar tungsten stimulating electrodes (Rhodes) were placed in the white matter to activate MF inputs to UBCs. In all experiments stimuli 100 μs in duration were employed, and all experiments were conducted in the presence of bicuculline (10 μM) to block γ-aminobutyric acid-A-receptor-mediated inhibitory synaptic currents. AMPA-receptor-mediated synaptic currents were recorded in the presence of bicuculline (10 μM) and the noncompetitive NMDA receptor antagonist 7-chlorokynurenic acid (50 μM).

Lucifer yellow (0.05%, K^+ salt, Molecular Probes) was included in the patch pipette in the majority of experiments to verify the identify of recorded neuron as a UBC on the basis of the characteristic morphology of the cell (Berthié and Axelrad 1994; Mugnaini and Floris 1994; Rossi et al. 1995). After the completion of whole cell or excised patch experiments, the morphology of the recorded neuron was viewed with the use of fluorescence attachments to the microscope.

Application of drugs

All drugs were dissolved in distilled water or dimethyl sulfoxide and applied by bath perfusion. The final concentration of dimethyl sulfoxide was always <1% in saline. The following compounds were used: bicuculline methobromide (Sigma), D−2-amino-5-phosphonovalerate (Tocris Cookson), cyclothiazide (generous gift of Eli Lilly, Indianapolis, IN), QX-314 (Alomone Laboratories), 7-chlorokynurenic acid (Tocris Cookson), L-*trans*-pyrrolidine-2,4-dicarboxylate (L-*trans*-PDC, Tocris Cookson), and 6-cyano-7-nitroquinoxaline-2,3-dione (CNQX, Tocris Cookson). Drugs were delivered to the bath by means of a peristaltic pump that fed initially into a premixing chamber above the microscope in which further gassing with 95% O_2-5% CO_2 was performed. Dose-response curves for the steady-state glutamate-activated current (I_{ss}) in outside-out patches were performed by the application of increasing [glu] by bath perfusion without washout between each dose. After exposure of the patch to the highest [glu] (1 mM), the patch was perfused with glutamate-free external solution; the use of the premixing chamber enabled a graded decline in [glu] to be achieved.

RESULTS

Experiments were conducted on >80 UBCs located in the granular layer of the nodulus and ventral uvula in thin rat cerebellar slices. UBCs were distinguished from adjacent granule cells by criteria previously described (Rossi et al. 1995), including their larger soma diameter (~9–13 μm), greater whole cell capacitance, prolonged synaptic response to single MF stimuli, and post hoc visualization of the cell morphology by fluorescent illumination of the Lucifer-yellow-filled cell after completion of the experiment. All experiments, unless otherwise noted, were performed in the presence of bicuculline (10 μM), 7-chlorokynurenic acid (50 μM), and raised extracellular Mg^{2+} (1.5 mM) at a holding potential of −80 mV to pharmacologically isolate the AMPA-receptor-mediated EPSC.

Time course of AMPA-receptor-mediated synaptic currents in UBCs

In the majority of cells examined, the time course of the AMPA-receptor-mediated EPSC in UBCs was biphasic, with a fast EPSC followed by a slow component that peaked in the range of 200–800 ms after the stimulus (Fig. 1*A*, Control). These two components of the EPSC may arise from the actions of glutamate at two independent receptor populations, or the complex time course of the synaptic current could arise from inherent properties of a single receptor population. To distinguish between these possibilities, the dose-dependent effects of cyclothiazide, which blocks AMPA receptor desensitization (Patneau et al. 1993; Trussell et al. 1993; Yamada and Tang 1993), was examined. Cyclothiazide produced a dose-dependent potentiation of the synaptic current at both early (Fig. 1*C*) and late (Fig. 1*D*) time periods (corrresponding to the peak of the fast and slow EPSCs in Fig. 1*A*, Control) and the total synaptic charge (Fig. 1*B*). Maximal effects of cyclothiazide were observed at 100 μM, with a depression of the response being observed at higher concentrations and a median effective dose of ~30 μM.

The synaptic current in the presence of cyclothiazide decayed smoothly, without evidence of a secondary component. This result would indicate that the slow EPSC does not arise from the actions of glutamate at receptors located at distant sites from that of release, because a potentiation of both components by cyclothiazide would be anticipated. Rather, the results support the contention that the time course of the AMPA-receptor-mediated EPSC is sculpted by an interplay between receptor properties and cleft [glu], as previously suggested (Rossi et al. 1995). Thus, when desensitization is blocked by cyclothiazide, the time course of the synaptic current will reflect the time course of [glu] in the synaptic cleft when this corresponds to the linear portion of the dose-response curve. In the majority of cells this decay could not be well fit with a single-exponential function. Fits of a double exponential to the time course of the current decay in 100 μM cyclothiazide for 12 cells yielded τ_f values of 58.3 ± 13.1 (SE) ms and τ_s values of 1,633.2 ± 261.6 ms.

In addition to blocking desensitization of AMPA receptors, cyclothiazide can slow deactivation kinetics (Patneau et al. 1993; Raman and Trussell 1995b), and it has been reported that the potentiation of AMPA-receptor-mediated EPSCs at small-diameter synapses may be due in part to an increase in presynaptic release (Diamond and Jahr 1995). A slowing of deactivation kinetics would be unlikely to contribute significantly to the very prolonged time course of synaptic currents in UBCs, but an enhancement in presynaptic release might contribute to the observed effects of cyclothiazide. One consequence of this would be to slow the rise time of the fast EPSC by disrupting the synchrony of release. Indeed, cyclothiazide produced a dose-dependent increase in the 10–90% rise time of the fast EPSC in UBCs (Fig. 2*A*, $n = 11$), but such an effect would also be expected for a blockade of fast desensitization alone. To further explore this, the effects of cyclothiazide were examined on NMDA-receptor-mediated EPSCs in UBCs. NMDA-receptor-mediated EPSCs were recorded in the absence of external Mg^{2+} and the presence of 10 μM CNQX to block AMPA receptors. In six cells, no statistically significant effect of cyclothiazide (100 μM) was observed on the total synaptic charge or time course of the EPSC, although a modest effect on the peak current was observed in four cells (Fig. 2*B*), which may reflect the direct postsynaptic actions of cyclothiazide previously observed in cultured hippocampal neurons (Diamond and Jahr 1995).

Dose dependence of steady-state glutamate currents in membrane patches

The proposed hypothesis regarding the cellular mechanism underlying the genesis of the slow AMPA-receptor-mediated EPSC in UBCs (Rossi et al. 1995; Slater et al. 1997a,b) hinges critically on the assumption that the steady-state dose-response relations for glutamate acting at AMPA receptors in UBCs is bell shaped. This has been previously reported for cultured cerebellar neurons (Geoffroy et al. 1991) and neurons of the chick nucleus magnocellularis (Raman and Trussell 1992), but has not been confirmed in cerebellar neurons in situ. To examine this, excised outside-out patches were obtained from the somata of both UBCs

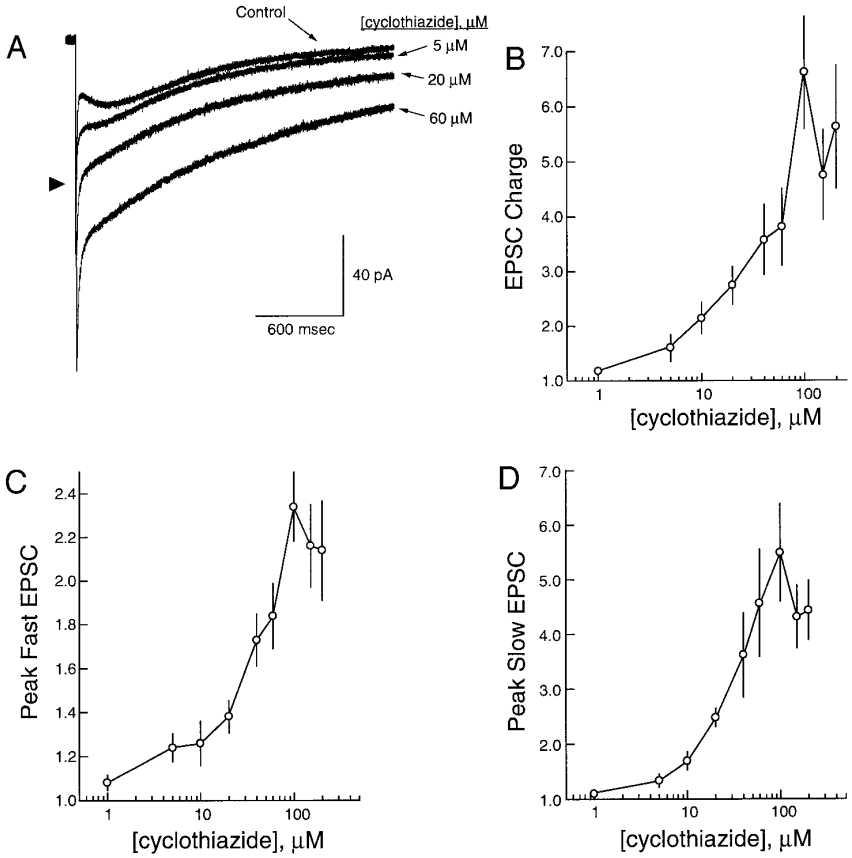

FIG. 1. Time course of the α-amino-3-hydroxy-5-methyl-4-isoxazolepropionic acid (AMPA)-receptor-mediated excitatory postsynaptic potential (EPSC) in unipolar brush cells (UBCs) and the dose-dependent modulation by cyclothiazide. *A*: AMPA-receptor-mediated synaptic currents in a rat UBC in the absence (Control) and presence of increasing concentrations of cyclothiazide, which blocks AMPA receptor desensitization. Each trace represents the average of 12 responses. Arrowhead: amplitude of the fast EPSC in Control. *B–D*: dose-dependent effects of cyclothiazide on the total synaptic charge (*B*), the peak amplitude of the fast EPSC (*C*), and the amplitude of the slow EPSC measured at a latency corresponding to the peak of the Control (*D*, 200 ms). All data have been normalized to their respective control synaptic currents and were derived from experiments with 11 UBCs.

and granule cells and the steady-state dose-response curve for glutamate was studied by bath application of glutamate (1 μM–1 mM) in the presence of bicuculline (10 μM), 7-chlorokynurenate (50 μM), and 1.5 mM external Mg^{2+}. In each experiment, the steady-state current at a given [glu] was normalized to that observed in the presence of 50 μM glutamate. In both UBCs (Fig. 3*A*) and granule cells (Fig. 3*C*) the steady-state dose-response curve was indeed bell shaped, with a maximal current being observed at 50 μM glutamate. These results would thus confirm the hypothesis that within 20–40 ms after release a ''quasi-steady-state'' [glu] is achieved (>50 μM) at the MF-UBC synapse in those cases in which a slow EPSC can be observed to follow a single stimulus, and the slow EPSC observed reflects this inherent property of AMPA receptors. If this is correct, then one should expect to observe a slow hump in the steady-state patch current when glutamate is washed gradually from the bath for patches from both cell types; this was also the case (Fig. 3, *B* and *D*). Thus the slow EPSC can be simulated in an excised somatic patch, and the properties of AMPA receptors in the synaptic cleft can be presumed to behave in a similar manner.

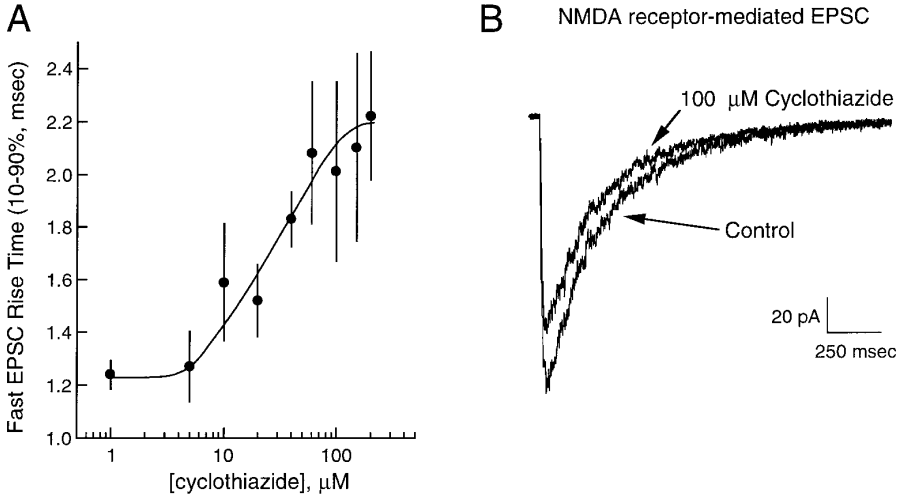

FIG. 2. Effects of cyclothiazide on EPSCs in UBCs. *A*: dose dependence of the effects of cyclothiazide on the 10–90% rise time of the AMPA-receptor-mediated EPSC in UBCs. *B*: effects of cyclothiazide on the *N*-methyl-D-aspartate (NMDA)-receptor-mediated EPSC in UBCs. Traces illustrate averaged NMDA-receptor-mediated synaptic currents in the absence (Control) and presence of 100 μM cyclothiazide. NMDA-receptor-mediated synaptic currents were pharmacologically isolated by recording in the presence of 10 μM 6-cyano-7-nitroquinoxaline-2,3-dione (CNQX) and 10 μM bicuculline.

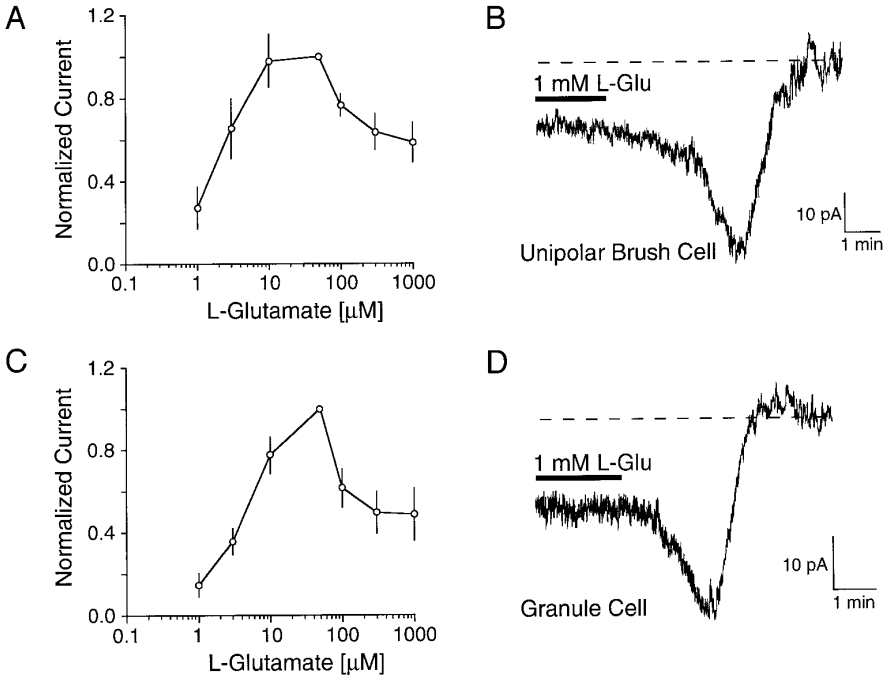

FIG. 3. Dose dependence of the steady-state AMPA-receptor-mediated current in excised outside-out patches from UBCs and granule cells. *A* and *C*: steady-state dose-response curves for glutamate acting on AMPA receptors in excised outside-out somatic patches obtained from UBCs (*A*) and granule cells (*C*). *B* and *D*: simulation of the slow EPSC. Steady-state glutamate current in an excised patch from a UBC (*B*) and granule cell (*D*) during the washout of 1 mM glutamate from the recording chamber to simulate the slow decline of glutamate concentration ([glu]) in a synaptic cleft. In patches from both cell types, a hump is observed during washout, which would be predicted from the steady-state dose-response curves (*left*). Data in *A* and *C* were normalized to the current at 50 μM; each point represents the mean ± SE of 5 patches. Experiments were conducted in the presence of 10 μM bicuculline, 50 μM 7-chlorokynurenate, and 1.5 mM external magnesium. Traces in *B* and *D* were filtered at 500 Hz for clarity of display.

It has been proposed that the reduction of the steady-state current at high [glu] originates from an accumulation of receptors in the desensitized state (Raman and Trussell 1992). To test this proposal, steady-state dose-response curves to glutamate were performed in excised outside-out patches from UBCs in the presence of 100 μM cyclothiazide (Fig. 4). Surprisingly, the dose-response relation in the presence of cyclothiazide was also bell shaped, with a peak current at 50 μM (Fig. 4, ○), and a hump in the current was also observed during washout of 1 mM glutamate (not shown), as in control patches from UBCs (Fig. 3*B*). However, in recordings from nucleated patches from UBCs in which potential effects of membrane stretch and cytoplasmic dialysis are reduced, cyclothiazide produced a dose-dependent potentiation of the glutamate-evoked current at concentrations >50 μM (Fig. 4, ■, ●), and no hump was observed during the washout of glutamate (Fig. 4, *inset*). These results support the suggestion that the reduction of the steady-state current at concentrations >50 μM arises from an accumulation of desensitized receptors.

Time course of [glu] in the synaptic cleft

Further validation of the glutamate entrapment hypothesis can be derived from experiments in which the [glu] in the synaptic cleft was directly manipulated. Several strategies were adopted to explore this. In the first series of experiments, a second MF stimulus was delivered at or near the peak of the slow EPSC. If the peak of the slow EPSC corresponds to a cleft [glu] of 50 μM, as the steady-state dose-response curve would suggest (Fig. 3*A*), then the second stimulus should drive the [glu] back into the millimolar range within the cleft, initially evoking a fast EPSC mediated by glutamate binding to unoccupied receptors. The hypothesis would predict that the peak of the fast EPSC evoked by the second stimulus should be smaller than that evoked by the first stimulus, because a fraction of the AMPA receptors will be already bound. Furthermore, the steady-state current following this will display an initial undershoot, reflecting the expected steady-state current at a higher cleft [glu]. These observations were all confirmed in paired-pulse experiments (n = 25), as illustrated in Fig. 5. Furthermore, the application of cyclothiazide (150 μM, n = 14) eliminated the undershoot observed to follow the second stimulus (Fig. 5*C*, ▼).

Paired-pulse experiments were also conducted as a means of exploring the time course of [glu] changes in the synaptic cleft and AMPA receptor occupancy. In 11 cells the interstimulus interval was systematically varied (50–2,000 ms) and the time-dependent changes in the peak amplitude of the fast EPSC and steady-state current evoked by the second stimulus were examined. An example of one experiment is illustrated in Fig. 6*A*. The peak amplitude of the fast EPSC evoked by the second MF stimulus is dramatically reduced at short interstimulus intervals. The amplitude of the fast EPSC evoked by the second MF stimulus will reflect the availability of unbound AMPA receptors in the synaptic cleft. At short interstimulus intervals many AMPA receptors will be already bound by glutamate, and thus the fast EPSC evoked by the test stimulus will be reduced. The peak of the fast EPSC to the test stimulus can thus be used as a probe for the availability of AMPA receptors in the cleft, and the fraction of bound (unavailable) receptors can be expressed as 1 − (test EPSC amplitude/1st EPSC amplitude). This fractional reduction in the test stimulus declines with time (Fig. 6*B*), indicative of the increasing availability of unbound AMPA receptors following the initial MF stimulus. This decline in the ratio of the fast EPSC amplitudes will thus reflect the time course of AMPA receptor occupancy (estimated here as the relative postsynaptic responsiveness),

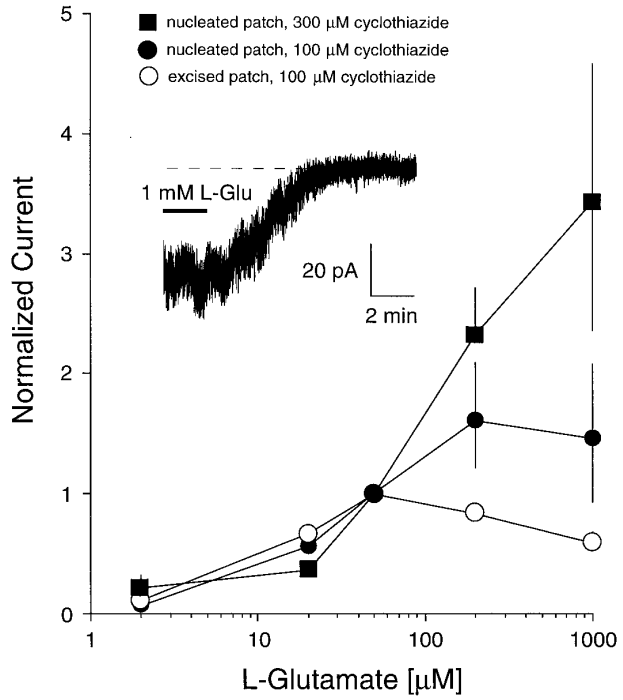

FIG. 4. Effects of cyclothiazide on the steady-state dose-response curves for glutamate acting on AMPA receptors in UBCs. Graph: biphasic steady-state dose-response curve for glutamate in an excised patch (○) compared with nucleated outside-out patches in the presence of 100 μM (●) or 300 μM (■) cyclothiazide. Cyclothiazide eliminated the reduction of the patch current at [glu] > 50 μM in nucleated patches in a dose-dependent manner, but was without effect in excised patches. *Inset*: current recorded in a nucleated patch in the presence of 100 μM cyclothiazide during the washout of 1 mM glutamate (cf. Fig. 3*B*). Note the absence of a hump in the current (cf. Fig. 3*B*) during washout. Current in *inset* was filtered at 500 Hz. Data in graph were normalized to the current at 50 μM; each point represents the mean ± SE of 4–7 patches. Experiments were conducted in the presence of 10 μM bicuculline, 50 μM 7-chlorokynurenate, and 1.5 mM external magnesium.

which in turn will be related to the time course of [glu] in the synaptic cleft. This rate of decline is similar to the rate of decay of the synaptic current in the presence of cyclothiazide (Fig. 1*A;* 10–90% decay time for EPSC in cyclothiazide = 2,070 ms, $n = 11$; 10–90% decay of fast EPSC ratio = 2,400 ms, $n = 11$). The decline in receptor occupancy estimated by paired-pulse experiments appears to approximate a single-exponential process (Fig. 6*B*) with a time constant of 800 ms and extinguishes at 5.4 s, the time at which no difference in the fast EPSC amplitudes was detected. Data were not obtained at short interstimulus intervals (<50 ms, to avoid significant changes in presynaptic release), and thus the results are not directly comparable with the initial decay of the synaptic current in the presence of cyclothiazide.

The undershoot of the ''steady-state current'' following the peak of the fast EPSC evoked by the second stimulus peaks at 40 ms in the majority of UBCs studied. Plots of the relationship between this steady-state current (measured 40 ms after the onset of the 2nd stimulus with respect to the baseline immediately preceding the second fast EPSC) and interstimulus interval yield the biphasic relation shown in Fig. 6*E*. The maximal amplitude of the undershoot, which would correspond to a cleft [glu] at the peak of the steady-state dose-response relation (50 μM, Fig. 3*A*) was observed at an interstimulus interval of 200 ms. The point in time at which this relation yields no net steady-state current is ~500 ms, a point in time that would correspond to a cleft [glu] on the rising slope of the steady-state dose-response curve producing a current equal to the maximum (~2.5 μM, Fig. 3*A*). Thus it can be estimated from these measures that the cleft [glu] transiently equilibrates at concentrations in the range of 0.4–1 mM 40 ms after release, falls to 50 μM at 200 ms and to 2.5 μM at 500 ms, and slowly declines to concentrations insufficient to activate ionotropic receptors over the course of 5–6 s.

In a third series of experiments the cleft [glu] was manipulated by lowering the extracellular calcium concentration. By decreasing the probability of release at any given site, the steady-state cleft [glu] may be reduced to a concentration <50 μM, whereon only a long tail should be observed following the fast EPSC. This prediction was also confirmed, as shown in Fig. 7*A*, where the slow EPSC was eliminated when the extracellular calcium concentration was reduced to 1.5 and 1.0 mM. In these experiments, the slow tail recorded at 1.0 mM extracellular calcium could then be reconverted into a slow EPSC by the delivery of a brief train of MF stimuli (200 Hz), which would presumably reflect a raised steady-state cleft [glu] of >50 μM (Fig. 7*B*).

In many UBCs, a single MF stimulus does not normally evoke a slow EPSC, but rather the fast EPSC is followed by a prolonged tail (Fig. 6*C* of Rossi et al. 1995). It has been suggested that the absence of a slow EPSC in these cells reflects a difference in synaptic morphology (Slater et al. 1997b). In some UBCs the area of synaptic apposition is not continuous, but is broken into numerous small contacts (Mugnaini et al. 1994; Rossi et al. 1995) reminiscent of calyceal synapses in the vestibular and auditory systems. Thus, after release at multiple sites, glutamate may escape by diffusion into a region having larger volume and lacking a high density of ionotropic receptors, resulting in a steady-state cleft [glu] <50 μM, and thus only a prolonged synaptic tail current is observed following the fast EPSC. In these cases, one might speculate that raising the levels of glutamate released may result in a raised steady-state cleft [glu] >50 μM, whereon a slow EPSC will be observed. To test this notion, brief repetitive MF stimuli (200 Hz) were applied and the responses of UBCs that displayed only synaptic tail currents to single stimuli (at 2.5 mM external calcium) were examined. In all cases examined (7 of 7), this resulted in the appearance of a slow EPSC, although the number of stimuli required to evoke a slow EPSC in any given cell varied (3–5 stimuli). An example of such an experiment is illustrated in Fig. 7*C*.

Paired-pulse experiments were also conducted in the presence of lowered extracellular calcium in five UBCs. The entrapment hypothesis would predict that when the cleft [glu] is lowered, a smaller fast EPSC and a reduction in the ratio of the EPSCs will be observed, the initial steady-state current (Fig. 8, arrowheads) will be larger if the cleft [glu] is nearer the peak of the dose-response curve, and the appearance of an undershoot in the current following the delivery of a second stimulus will be abolished. These predictions were confirmed, as illustrated in Fig. 8, *A* and *B*. In UBCs

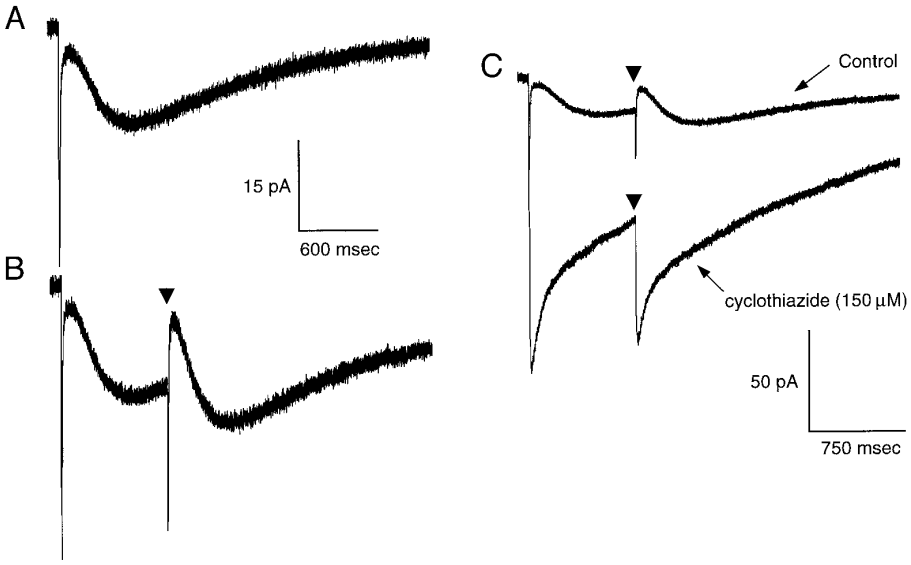

FIG. 5. Paired-pulse experiments confirm the hypothesis that the slow EPSC arises from a steady-state current. *A*: averaged AMPA-receptor-mediated synaptic current in a UBC in response to single mossy fiber (MF) stimuli. *B*: responses of the same cell in which a 2nd MF stimulus was delivered just after the peak of the slow EPSC (▼, interstimulus interval 800 ms). Note the reduction in the amplitude of the fast EPSC in response to the 2nd stimulus and the pronounced undershoot of the current that follows. *C*: effects of cyclothiazide on the synaptic current evoked by paired stimuli. *Top trace* (Control) is the same trace shown in *B* at a lower vertical gain; *bottom trace* is the averaged synaptic current following the application of cyclothiazide (150 μM). In the presence of cyclothiazide, no slow EPSC is observed (see also Fig. 1), and the undershoot following the 2nd stimulus is abolished (▼).

in which a slow EPSC was still present in lowered external calcium, such as that illustrated in Fig. 8, the latency-to-peak of the slow EPSC was reduced, presumably reflecting the decreased cleft [glu], which will require less time to decline to the peak of the steady-state dose-response curve. Furthermore, delivery of a brief paired stimulus train to evoke more glutamate release also restored the undershoot following the second stimulus in lowered external calcium (Fig. 8*C*) as well as enhancing the amplitude of the slow EPSC and reducing the initial steady-state current.

Role of glutamate transport

The very slow time course of the synaptic current in UBCs raises the possibility that glutamate reuptake may contribute to the removal of glutamate from the synaptic cleft. To assess the contribution of glutamate reuptake to the time course of the EPSC in UBCs, the effects of the competitive glutamate transport inhibitor L-*trans*-PDC (Bridges et al. 1991) on the time course of the AMPA-receptor-mediated EPSC were examined. In the presence of 100 μM L-*trans*-PDC, a prolon-

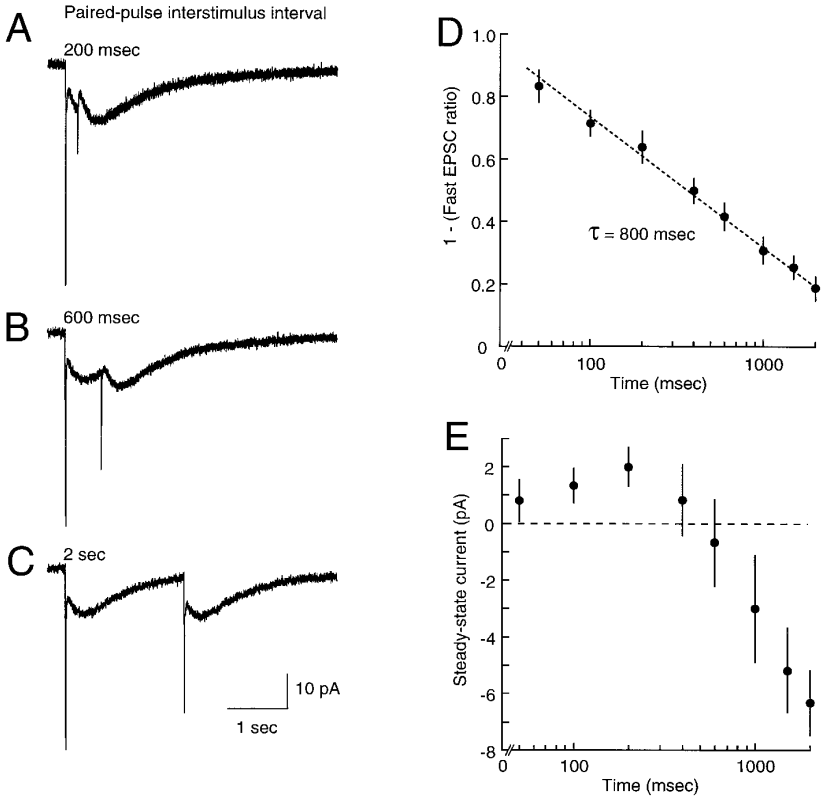

FIG. 6. Paired-pulse experiments suggest a long-lasting occupancy of AMPA receptors following MF stimulation. *A–C*: synaptic currents evoked by paired MF stimuli delivered at the indicated interstimulus intervals. *D*: assessment of the decline in AMPA receptor occupancy following glutamate release. Graph shows a semilogarithmic plot of the decline in the difference between the ratio of the fast EPSC evoked by paired MF stimuli, expressed as 1 − (test EPSC amplitude/1st EPSC amplitude). Ratio declines with a time constant of 800 ms and decays to 0 at 5.4 s. *E*: plot of the amplitude of the initial steady-state current with interstimulus interval. Steady-state current was measured 40 ms after the onset of the 2nd stimulus with respect to the baseline immediately preceding this stimulus. At short intervals (50–400 ms) the initial steady-state current is positive (*A*), reflecting an undershoot in the current, which reverses between 400 and 600 ms (*B*) and gradually recovers to negative values after several s (*C*). These results, taken together with those presented in Fig. 3, allow predictions to be made regarding the time course of decline of glutamate levels in the synaptic cleft following release (see text).

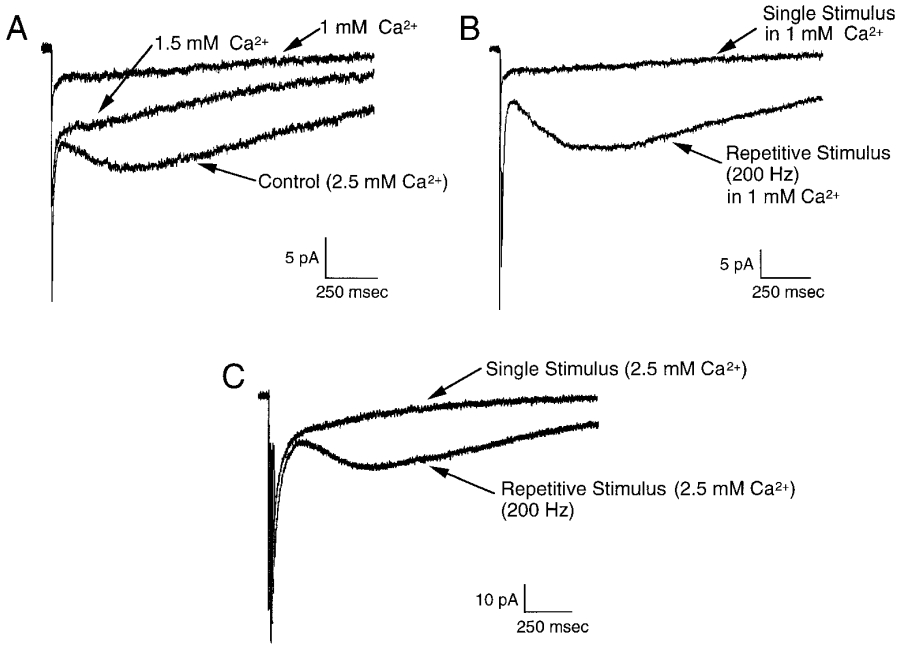

FIG. 7. Modulation of presynaptic release probability affects the amplitude of the slow EPSC. *A*: AMPA-receptor-mediated synaptic currents in a UBC recorded at 2.5 (Control), 1.5, and 1.0 mM external calcium. Traces are averaged responses to single MF stimuli at each external [calcium]. Note the abolition of the slow EPSC by lowered external calcium. *B*: slow EPSC at a lowered external calcium concentration (1 mM) is restored by delivery of a brief stimulus train (3 stimuli 100 μs in duration at 200 Hz). *C*: AMPA-receptor-mediated synaptic currents in some UBCs recorded in the presence of 2.5 mM external calcium lack a slow EPSC and display only a prolonged tail current in response to single MF stimuli (single stimulus). Slow EPSC can be revealed in these cells by the application of a brief stimulus train (repetitive stimulus, 5 stimuli 100 μs in duration at 200 Hz).

gation of the late component of the EPSC was observed, as well as an increase in the total charge in 12 of 15 cells studied (36 ± 6%, $P < 0.05$), despite a decrease in the amplitude of the fast EPSC in all cells (24 ± 6% decrease, Fig. 9). These effects were readily reversible on washout of L-*trans*-PDC. In contrast to the effects of L-*trans*-PDC in other neurons (Barbour et al. 1994; Isaacson and Nicoll 1993; Sarantis et al. 1993; Takahashi et al. 1995), no significant inward current was produced by L-*trans*-PDC in UBCs. However, these studies employed higher concentrations of L-*trans*-PDC (300–500 μM); when a higher dose of L-*trans*-PDC (300 μM) was applied to UBCs, the synaptic current was almost completely blocked. When 100 μM L-*trans*-PDC was applied in the presence of cyclothiazide (100 μM), the fast EPSC amplitude was reduced (17% ± 5%), with a concomitant increase (33 ± 17%) in the total charge in 7 of 10 cells and prolongation of the time course of the slow EPSC (10–90% decay time in cyclothiazide alone: 2,070 ± 247 ms; cyclothiazide + L-*trans*-PDC: 3,076 ± 376 ms; $P < 0.05$).

DISCUSSION

Time course of glutamate in the MF-UC synaptic cleft

A number of lines of evidence support the hypothesis that glutamate remains entrapped in the MF-UBC synapse for prolonged periods of time and that the resulting EPSC is produced by the repeated binding and unbinding of transmitter to postsynaptic receptors. These include *1*) the slow time course of the AMPA component when desensitization is blocked by cyclothiazide (Fig. 1), *2*) the time course of changes in synaptic conductance, which mirror the time course of the synaptic current estimated in voltage jump experiments (Rossi et al. 1995), *3*) paired-pulse experiments displaying a prolonged reduction of the amplitude of the fast EPSC evoked by a second MF stimulus, indicative of prolonged occupancy of postsynaptic receptors following a single stimulus (Fig. 6), and *4*) the steady-state dose-response data, which predict the time course of the slow EPSC and changes in the EPSC waveform with paired stimuli and reduced release. This situation is dramatically different from that in other glutamatergic synapses, where the lifetime of glutamate has been estimated from rapid perfusion experiments (see Jonas and Spruston 1994 for review) and the effects of competitive antagonists (Clements 1996; Clements et al. 1992) to be very brief (1–2 ms), and thus the fast AMPA component of the EPSC declines rapidly without significant rebinding of glutamate (Clements 1996; Edmonds et al. 1995; Jonas and Spruston 1994; Jones and Westbrook 1996). Deactivation appears to be the predominant factor in sculpting the decay of the fast EPSC, but desensitization may also be important at other giant synapses when the release probability is high (Trussell et al. 1993).

Data regarding the dose dependence of the steady-state current in UBCs (Fig. 3*A*) and the synaptic currents evoked by paired stimuli (Fig. 6) allow estimates to be made of the time course of glutamate within the synaptic cleft and the mechanism by which the slow EPSC is produced. This is schematically illustrated in Fig. 10. It can be assumed that glutamate released at individual sites transiently achieves a concentration at the postsynaptic membrane in the low millimolar range within 50 μs, as in other glutamatergic synapses (Clements 1996). The concentration will then decline rapidly to equilibrate between cleft compartments (Fig. 10*A*). At ~40 ms a steady-state current is achieved (labeled *a* in Fig. 10, *A* and *B*); this current gradually rises in amplitude as the [glu] further declines by diffusional escape from the edges of the synaptic matrix, giving rise to the observed slow EPSC. A peak is generally observed at ~200 ms, which would correspond to the peak of the biphasic dose-response curve for the steady-state current (labeled *b* in Fig. 10*C*). With the further decline in [glu] the slow EPSC will first

reach a value equal to the initial equilibrium value (labeled *c* in Fig. 10, *B* and *C*) and then decay to the holding current. In paired-pulse experiments, maximal values of the undershoot are observed when the second stimulus is applied at the peak of the slow EPSC (labeled *b* in Fig. 10, *B–D*), which would correspond to the maximal drop in I_{ss} expected if the surge of additional glutamate into the cleft by the second stimulus reequilibrated at maximal values (difference between *b* and *a* in Fig. 10*C*). Because maximal values of I_{ss} and the undershoot were observed at 50 μM glutamate and 200-ms intervals, respectively, the data would suggest that cleft [glu] falls to 50 μM at 200 ms. In paired-pulse experiments the initial values of I_{ss} reverse at intervals of ~500 ms, which would correspond to a concentration of 2.5 μM glutamate estimated from the dose-response relations for I_{ss} (labeled *c* in Fig. 10, *C* and *D*). At this time interval the second fast EPSC is reduced by ~50%. It has been shown that a low [glu] induces AMPA receptor desensitization that inhibits the response to a subsequent high [glu] or a synaptic stimulation with a median inhibiting concentration in the range of 1–10 μM (Colquhoun et al. 1992). Thus our estimate of 2.5 μM at the time (500 ms) at which a 50% reduction in the fast EPSC occurs fits well with the data of Colquhoun et al. (1992). AMPA receptor occupancy, estimated by the ratio of fast EPSCs evoked by paired stimuli (Fig. 6), declines with a time constant of 800 ms to zero at 5.4 s, which is similar to the rate of decay of the EPSC in the presence of cyclothiazide (Fig. 1).

There are several important caveats to these estimates of the time course of [glu] in the cleft. One is that presynaptic contributions to the changes in EPSCs are ignored. MF-evoked EPSCs in granule cells (which are postsynaptic to the same terminals as UBCs) generally display paired-pulse depression, but the time course of recovery of this has not been examined. Thus it is possible that some contribution of changes in presynaptic release may extend beyond 50 ms. Another consideration is that the synaptic ultrastructure of the MF-UBC synapse is highly variable, and the estimates above pertain only to the cell popuation studied here. Many UBCs display only a slow tail of AMPA current (e.g., Fig. 7*C*), whereas in others the time-to-peak of the slow component may be as long as 1 s (not shown). Finally, it must be borne in mind that

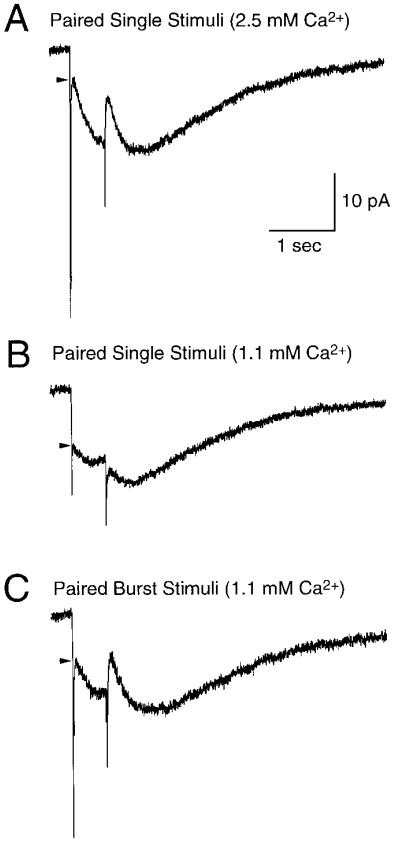

FIG. 8. Paired-pulse experiments in lowered extracellular calcium. *A*: AMPA-receptor-mediated EPSC evoked by paired single stimuli in the presence of 2.5 mM external calcium. Second stimulus was delivered at the peak of the slow EPSC (interstimulus interval 500 ms), producing an undershoot of the steady-state current *B*: synaptic current in the same cell evoked by paired single stimuli in the presence of a lowered (1.1 mM) external calcium concentration. *C*: restoration of the undershoot evoked by the 2nd stimulus in the presence of lowered external calcium (1.1 mM) by delivery of a pair of brief stimulus trains (6 stimuli 100 μs in duration at 200 Hz). For clarity of presentation, the current before and after each fast EPSC was filtered at 200 Hz. Arrowheads: amplitude of the initial steady-state current 40 ms after the stimulus.

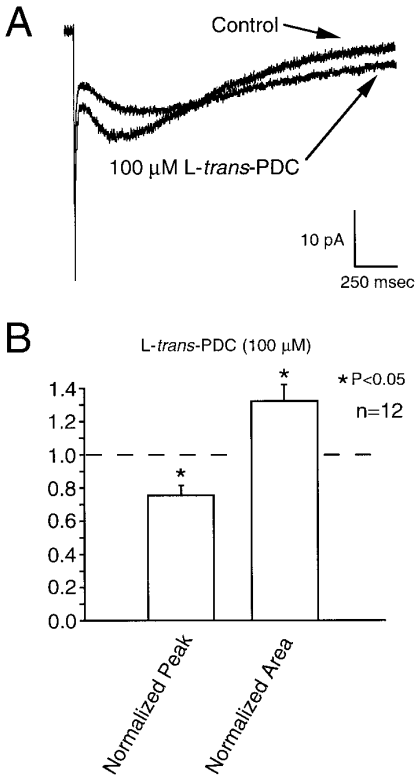

FIG. 9. Actions of the glutamate reuptake inhibitor L-*trans*-pyrrolidine-2,4-dicarboxylate (L-*trans*-PDC) on the biphasic AMPA-receptor-mediated EPSC in UBCs. *A*: time course of the AMPA-receptor-mediated EPSC in a UBC before (Control) and after the application of 100 μM L-*trans*-PDC. *B*: histogram of the normalized effects of L-*trans*-PDC on the peak of the fast EPSC (normalized peak) and the total synaptic charge (normalized area) for 12 UBCs. Note the prolongation of duration (*A*) and consequent increase in total charge (*B*) produced by L-*trans*-PDC despite the significant reduction in the amplitude of the fast and slow components of the EPSC.

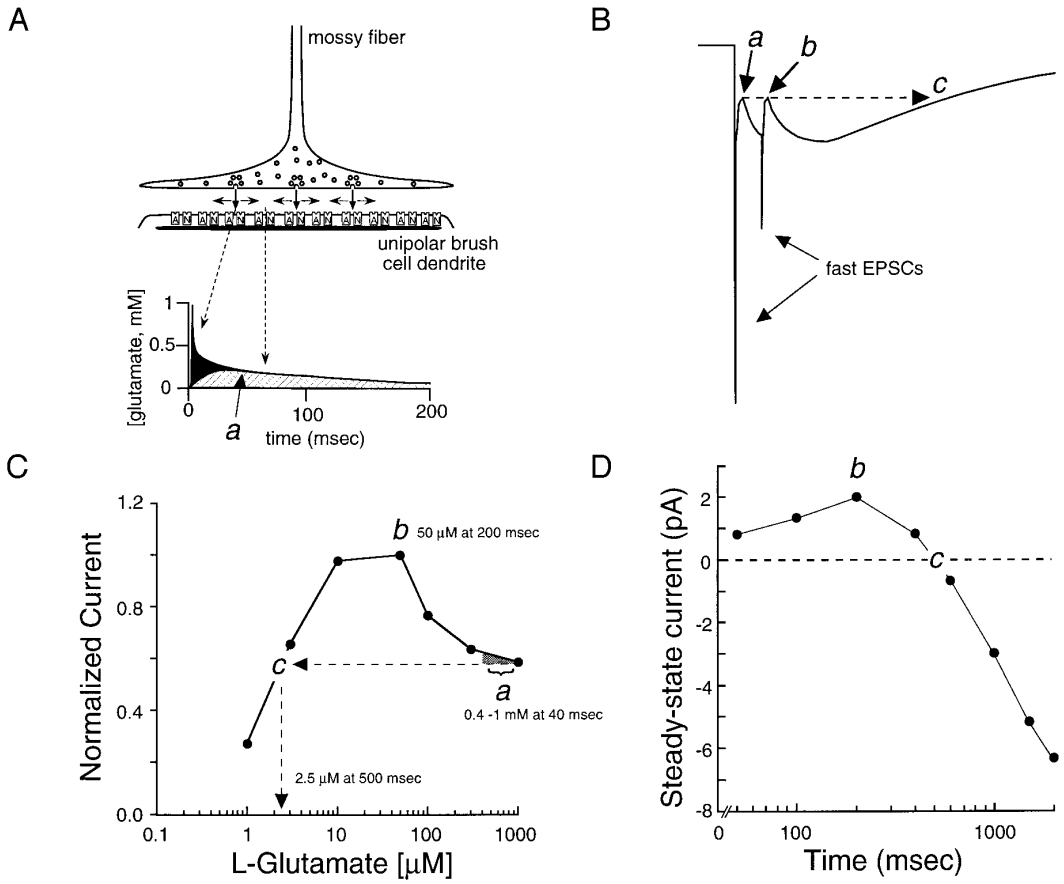

FIG. 10. Schematic illustration of the cellular mechanism of the biphasic AMPA-receptor-mediated EPSC in UBCs. *A*: schematic illustration of the ultrastructural features of the MF-UBC synapse (*top*), showing multiple release sites and the continuous distribution of ionotropic AMPA (A) and NMDA (N) receptors on the postsynaptic density. *A, bottom*: proposed slow decline of cleft [glu] during the 1st 200 ms, with equilibration between the 2 synaptic compartments occurring at the time labeled *a* (~40 ms after the onset of release). Filled area of graph: [glu] within cleft compartments immediately apposed to release sites. Hatched area: compartments between release sites. *B–D*: diagram of the idealized synaptic current mediated via AMPA receptors in response to paired single stimuli (*B*), the dose-response relations for the steady-state current (*C*, derived from Fig. 3*A*), and the change in amplitude and polarity of the slow synaptic current (*D*, derived from Fig. 6*E*) to illustrate the mechanism of the AMPA-receptor-mediated synaptic current in UBCs. The first MF stimulus evokes a current that peaks and then rapidly decays to an initial steady state after ~40 ms (labeled *a* in *B* and *C*). Synaptic current then rises to the peak of the slow EPSC as cleft [glu] falls and the peak of the dose-response curve for the steady-state current is reached (labeled *b* in *C–D*). Delivery of a 2nd stimulus at this point evokes a 2nd fast EPSC of reduced amplitude followed by an undershoot of the steady-state current (labeled *b* in *B*) as cleft [glu] reequilibrates at a higher level, which will produce a smaller current (from *b* to *a* in *C*). After the undershoot a slow EPSC reemerges with the decline in cleft [glu], decays to a level equal to the current immediately after the fast EPSC (labeled *c* in *B–D*), and finally decays to zero as glutamate levels fall to ineffective concentrations within the cleft.

the time course of the EPSC in any individual cell reflects the sum of changes at each region of synaptic apposition, and these vary greatly in size. Thus the total synaptic current will reflect both fast and slow EPSCs generated at individual regions of apposition.

A central requirement of the glutamate entrapment hypothesis (Rossi et al. 1995; Slater et al. 1997b) is that significant steady-state currents are generated at the postsynaptic membrane. Steady-state currents of this magnitude (10–30 pA) are not generally observed in rapid perfusion experiments employing excised patches derived from somatic membrane. This discrepancy may be explained if AMPA receptors at the subsynaptic membrane display gating properties different from those at nonsynaptic locations, and indeed, NMDA receptors appear to be tethered to filamentous actin (Rosenmund and Westbrook 1993) and A-kinase-anchoring proteins tether protein kinase A, which modulates the gating of AMPA receptors (Rosenmund et al. 1994). Furthermore, with the use of both rapid perfusion techniques and flash photolysis of caged glutamate, it has been shown that the fractional steady-state AMPA current is larger in intact cells when compared with excised patches from the same cell type (Margulis and Tang 1996; Raman and Trussell 1992). Alternative hypotheses for the generation of the slow EPSC, such as a secondary metabotropic-glutamate-receptor-mediated EPSC (Batchelor et al. 1994), are not compatible with the observed undershoot of the current in paired-pulse experiments (Figs. 5 and 6) or the CNQX sensitivity of this component (Rossi et al. 1995).

Contribution of desensitization to the time course of the synaptic current

The present data indicate that the complex three-dimensional geometry of the MF-UBC synaptic cleft acts to effectively entrap glutamate after release at multiple sites for very prolonged periods (5–6 s, see preceding text). The abolition of the slow EPSC and overall enhancement of the EPSC by cyclothiazide (Fig. 1) suggests that desensitization strongly contributes to the time course of the EPSC, because cyclothiazide blocks AMPA receptor desensitization, and thus the synaptic current in the presence of cyclothiazide will approximate the time course of receptor occupancy. Because AMPA receptors have a low affinity for glutamate (Patneau and Mayer 1990), the time course of the AMPA current will somewhat underestimate the lifetime of glutamate at this synapse. However, these estimates are further complicated by other actions of cyclothiazide not related to the blockade of desensitization of the AMPA receptor, such as a slowing of deactivation kinetics (Patneau et al. 1993; Raman and Trussell 1995b) and presynaptic enhancement of glutamate release via desynchrony of release and an increase in release probability (Diamond and Jahr 1995). A slowing of glutamate dissociation from the AMPA receptor would result in a prolonged EPSC, but it should be noted that the NMDA-receptor-mediated component lasts for several seconds, despite desensitization, and it can be speculated that glutamate lasts for periods of up to 5 s at least (Fig. 6*D*). An enhancement of presynaptic glutamate release by cyclothiazide would be unlikely to significantly contribute to the time course of the AMPA current in cyclothiazide over the long time scale of the EPSC, because NMDA-receptor-mediated synaptic currents in the presence of cyclothiazide were not prolonged in duration (Fig. 2*B*). Some contribution by a presynaptic action of cyclothiazide to the peak current would be expected, however. An analysis of the effects of cyclothiazide on miniature EPSCs would be useful in this regard, but spontaneous miniature EPSCs are rare in UBCs, and we have thus far been unable to provoke miniature EPSCs by the application of α-latrotoxin (Fesce et al. 1986; Grasso and Mercanti-Ciotti 1993) or hyperosmotic solutions (Bekkers and Stevens 1995).

The observation that cyclothiazide was without effect in excised patches from UBCs, but was effective in nucleated patches, indicates that the process of patch excision abolished the ability of cyclothiazide to block desensitization. This result is surprising, because a blockade of AMPA receptor desensitization by cyclothiazide in excised patches has been observed in other neurons (e.g., Arai and Lynch 1996; Bertolino et al. 1993; Eliasof and Jahr 1997; Partin et al. 1996). Cyclothiazide binds to serine residues at position 750 in an extracellular loop of AMPA receptors to inhibit desensitization (Partin et al. 1995, 1996). The elimination of cyclothiazide sensitivity by patch excision in UBCs would suggest that intracellular factors necessary for the action of cyclothiazide are disrupted. UBCs possess a dense subsynaptic web that is devoid of neurofilaments (Harris et al. 1993; Mugnaini et al. 1994) and enriched in filamentous actin (Diño et al. 1996). The elimination of cyclothiazide sensitivity by patch excision may arise from the disruption of filamentous actin tethered to AMPA receptors at nonsynaptic sites, by dialysis of intracellular messengers, or by membrane stretch during the excision process, which can modulate glutamate receptor channel properties (Zhang et al. 1996).

Contribution of glutamate reuptake

The failure of reuptake blockers to significantly potentiate AMPA-receptor-mediated synaptic currents at some synapses (Hestrin et al. 1990; Isaacson and Nicoll 1993; Sarantis et al. 1993) has been interpreted as evidence that the clearance of glutamate from the synaptic cleft occurs predominantly by diffusion. A contribution of reuptake can be seen at synapses with multiple release sites, such as UBCs (Fig. 9) and calyceal synapses (Otis et al. 1996), and in cases in which significant ''cross talk'' may occur between densely packed individual terminals (Barbour et al. 1994; Mennerick and Zorumski 1995; Takahashi et al. 1995). In glomerular synapses of the cerebellum, the escape of glutamate from the cleft at MF-UBC and MF–granule cell synapses must take place by diffusion through a labyrinthine three-dimensional volume formed by densely packed UBC, granule cell, and Golgi cell dendritic processes ~3–4 μm in cross-sectional distance (Jakab 1989; Jakab and Hámori 1988; Mugnaini 1972; Palay and Chan-Palay 1974). However, the diffusional flux of glutamate will be further limited by extracellular tortuosity (λ), which in the cerebellar granular layer has a mean value of 1.7 (Krizaj et al. 1996). Glutamate transporters are localized primarily to glial cell membranes that envelop this complex glomerular space (Chaudhry et al. 1995; Storm-Mathisen et al. 1995). Thus the distance from the synaptic cleft to areas of extracellular space in which reuptake will significantly buffer glutamate levels is considerable (5–8 μm, corrected for λ). In the case of cerebellar granule cells, reuptake inhibitors do not produce a marked prolongation of the decay of the fast EPSC (Sarantis et al. 1993), although a significant effect is seen in these cells during repetitive activation of MFs (Slater and Kinney 1996). In UBCs, however, the effects of reuptake blockade are readily observed to single afferent stimuli (Fig. 9); this would infer that the diffusional escape of glutamate at this synapse is sufficiently slow that glial reuptake effectively regulates the concentration gradient within the glomerular volume and thus influences the diffusional flux of glutamate from the synaptic cleft.

The reduction of amplitude of the fast and slow components of the EPSC in the presence of L-*trans*-PDC may result from cross-desensitization of synaptic AMPA receptors by elevated extracellular glutamate levels. In other neuronal cells this is accompanied by an inward current (Barbour et al. 1994; Isaacson and Nicoll 1993; Sarantis et al. 1993; Takahashi et al. 1995), but inward currents were not observed in UBCs at a concentration (100 μM) sufficient to produce a reduction of the EPSC amplitude. Thus the raised extracellular glutamate levels may act to depress glutamate release via activation of presynaptic metabotropic glutamate receptors (Maki et al. 1994), which is consistent with the observed reduction of EPSCs by L-*trans*-PDC when desensitization was blocked by cyclothiazide.

Giant synapses and synaptic transmission

Giant glutamatergic synapses are found in both the peripheral and central circuitry of the auditory and vestibular systems and fall into two major classes, the well-described calyceal synapses and the more recently discovered MF-UBC type. Giant calyceal synapses within central and peripheral auditory and vestibular circuits share some similarities with the MF-UBC synapse in that both classes of synapse have multiple release sites and there is a large area of apposition of pre- and postsynaptic membrane (e.g., Mattox et al. 1985; Mugnaini et al. 1994; Parks et al. 1990; Wright et al. 1996). Thus a high degree of synchrony of presynaptic release of transmitter will be achieved, which will be of functional importance in these pathways. However, the presynaptic terminal at calyceal synapses forms a network of individual digitiform contacts, apposed to which clusters of glutamate receptors are found (Dememes et al. 1995) and between which glutamate can more rapidly escape to extracellular space. At these synapses, glutamate may persist within the cleft of individual contacts for relatively prolonged periods, but only at levels of concentration sufficient to produce a very small late component of the EPSC (Otis et al. 1996). Thus the EPSC at calyceal synapses is much faster in time course than that in UBCs, an adaptation that is of importance in high-frequency following of vestibular and auditory sensory input.

The functional importance of the synaptic specialization in UBCs is presently unknown. UBCs occur both in central vestibular pathways of the cerebellum (Altman and Bayer 1977; Floris et al. 1994; Mugnaini and Floris 1994) and in the dorsal cochlear nucleus (Floris et al. 1994; Wright et al. 1996), but the origin of the MFs that innervate them has not been identified. MFs innervating UBCs of the dorsal cochlear nucleus may arise from the cuneate region (Wright and Ryugo 1996). Although a subset of cerebellar UBCs in the nodulus receives cholinergic MFs, which likely arise from the medial vestibular nucleus (Jaarsma et al. 1996), many are directly innervated by primary vestibular fibers of the eighth nerve (Diño et al. 1997), which may represent one source of glutamatergic afferents to these cells. Cerebellar UBCs give rise to an axon that branches within the granular layer, giving rise to terminals that likely innervate a subset of granule cells (Berthié and Axelrad 1994; Rossi et al. 1995; Slater et al. 1997b). A single action potential in the MF innervating a cerebellar UBC may thus drive a train of EPSCs in a large ensemble of granule cells. The elucidation of the circuitry within which UBCs reside and the physiological conditions for the activation of these unique cells in vivo represent important goals for future research.

What is the functional role of the slow AMPA-receptor-mediated synaptic current in UBCs? In most UBCs the net synaptic charge in the absence of external magnesium is dominated by the NMDA component and the fast AMPA-receptor-mediated component is thought to function primarily to charge membrane capacitance (Rossi et al. 1995). Under physiological conditions, external magnesium will block NMDA receptor channels at the resting potential and the AMPA-receptor-mediated component will function in two ways. First, the fast EPSP will depolarize the membrane into a region that relieves magnesium channel block and enables the expression of the NMDA-receptor-mediated component. Second, the slow AMPA-receptor-mediated EPSC will function as positive feedback to maintain the depolarization. This will be most effective in cells that display a prominent slow EPSC, but the high input resistance of the UBC will require only small amounts of synaptic current to generate a significant depolarization, and thus UBCs displaying only a small tail current will also be effective in this regard. The generation of slow AMPA-receptor-mediated EPSCs in all UBCs by brief repetitive stimuli has important physiological implications in that high-frequency bursts of afferent activity are normally observed in MFs in vivo (Bauswein et al. 1984; van Kan et al. 1993). Thus bursts of MF activity will preferentially produce a sustained train of postsynaptic action potentials arising from the facilitation of the slow AMPA-receptor-mediated EPSC as well as temporal summation of the NMDA-receptor-mediated EPSC in UBCs.

We are grateful to Drs. S. Alford, M. Haüsser, S. Hestrin, E. Mugnaini, C. Nicholson, N. Spruston, and L. O. Trussell for helpful discussions during the course of this work and to Drs. K. E. McKenna and R. J. Schuerger for reading the manuscript.

This work was supported by National Institutes of Health Grants NS-34840 and DC-002764 to N. T. Slater.

Address for reprint requests: N. T. Slater, Dept. of Physiology M211, Northwestern University Medical School, 303 E. Chicago Ave., Chicago, IL 60611.

Received 24 July 1996; accepted in final form 13 May 1997.

REFERENCES

Altman, J. and Bayer, S. A. Time of origin and distribution of a new cell type in the rat cerebellar cortex. *Exp. Brain Res.* 29: 265–274, 1977.

Arai, A. and Lynch, G. Response to repetitive stimulation of AMPA receptors in patches excised from fields CA1 and CA3 of the hippocampus. *Brain Res.* 716: 202–206, 1996.

Barbour, B., Keller, B. U., Llano, I., and Marty, A. Prolonged presence of glutamate during excitatory synaptic transmission to cerebellar Purkinje cells. *Neuron* 12: 1331–1343, 1994.

Batchelor, A. M., Madge, D. J., and Garthwaite, J. Synaptic activation of metabotropic glutamate receptors in the parallel fibre–Purkinje cell pathway in rat cerebellar slices. *Neuroscience* 63: 911–915, 1994.

Bauswein, E., Kolb, F. P., and Rubia, F. J. Cerebellar feedback signals of a passive hand movement in the awake monkey. *Pflügers Arch.* 402: 292–299, 1984.

Bekkers, J. M. and Stevens, C. F. Quantal analysis of EPSCs recorded from small numbers of synapses in hippocampal cultures. *J. Neurophysiol.* 73: 1145–1156, 1995.

Berthié, B. and Axelrad, H. Granular layer collaterals of the unipolar brush cell axon display rosette-like excrescences. A Golgi study in the rat cerebellar cortex. *Neurosci. Lett.* 167: 161–165, 1994.

Bertolino, M., Baraldi, M., Parenti, C., Braghiroli, D., DiBella, M., Vicini, S., and Costa, E. Modulation of AMPA/kainate receptors by analogues of diazoxide and cyclothiazide in thin slices of rat hippocampus. *Receptors Channels* 1: 267–278, 1993.

Bridges, R. J., Stanley, M. S., Anderson, M. W., Cotman, C. W., and Chamberlain, A. R. Conformationally defined neurotransmitter analogues: selective inhibition of glutamate uptake by one pyrrolidine-2,4-dicarboxylate diasteromer. *J. Med. Chem.* 34: 717–725, 1991.

Chaudhry, F. A., Lehre, K. P., van Lookeren Campagne, M., Ottersen, O. P., Danbolt, N. C., and Storm-Mathisen, J. Glutamate transporters in glial plasma membranes: highly differentiated localizations revealed by quantitative ultrastructural immunocytochemistry. *Neuron* 15: 711–720, 1995.

Clements, J. D. Transmitter timecourse in the synaptic cleft: its role in central synaptic function. *Trends Neurosci.* 19: 163–171, 1996.

CLEMENTS, J. D., LESTER, R.A.J., TONG, G., JAHR, C. E., AND WESTBROOK, G. L. The time course of glutamate in the synaptic cleft. *Science* 258: 1498–1501, 1992.

COLLINGRIDGE, G. L. AND LESTER, R.A.J. Excitatory amino acids in the vertebrate central nervous system. *Pharmacol. Rev.* 40: 143–210, 1990.

COLQUHOUN, D., JONAS, P., AND SAKMANN, B. Action of brief pulses of glutamate on AMPA/kainate receptors in patches from different neurones of rat hippocampal slices. *J. Physiol. (Lond.)* 458: 261–287, 1992.

D'ANGELO, E., ROSSI, P., AND TAGLIETTI, V. Different proportions of *N*-methyl-D-aspartate and non-*N*-methyl-D-aspartate receptor currents at the mossy fibre–granule cell synapse of developing rat cerebellum. *Neuroscience* 53: 121–130, 1993.

DEMEMES, D., LLEIXA, A., AND DECHESNE, C. J. Cellular and subcellular localization of AMPA-selective glutamate receptors in the mammalian peripheral vestibular system. *Brain Res.* 671: 83–94, 1995.

DIAMOND, J. S. AND JAHR, C. E. Asynchronous release of synaptic vesicles determines the time course of the AMPA receptor-mediated EPSC. *Neuron* 15: 1097–1107, 1995.

DIÑO, M. R., SEKERKOVA, G., CUNHA, S., BINDER, L., AND MUGNAINI, E. The cytoskeleton of unipolar brush cells of the mammalian cerebellum. *Soc. Neurosci. Abstr.* 22: 1631, 1996.

DIÑO, M. R., SEKERKOVA, G., PERACHIO, A. A., AND MUGNAINI, E. Unipolar brush cells are targets of primary vestibular fibers. *Soc. Neurosci. Abstr.* In press.

EBRALIDZE, A. K., ROSSI, D. J., TONEGAWA, S., AND SLATER, N. T. Modification of NMDA receptor-channels and synaptic transmission by targeted disruption of the NR2C gene. *J. Neurosci.* 16: 5014–5025, 1996.

EDMONDS, B., GIBB, A. J., AND COLQUHOUN, D. Mechanisms of activation of glutamate receptors and the time course of excitatory synaptic currents. *Annu. Rev. Physiol.* 57: 495–519, 1995.

EDWARDS, F. A., KONNERTH, A., SAKMANN, B., AND TAKAHASHI, T. A thin slice preparation for patch clamp recordings from neurones of the mammalian central nervous system. *Pflügers Arch.* 414: 600–612, 1989.

ELIASOF, S. AND JAHR, C. E. Rapid AMPA receptor desensitization in catfish cone horizontal cells. *Visual Neurosci.* 14: 13–18, 1997.

FESCE, R., SEGAL, J. R., CECCARELLI, B., AND HURLBUT, W. P. Effects of black widow spider venom and Ca^{2+} on quantal secretion at the frog neuromuscular junction. *J. Gen Physiol.* 88: 59–81, 1986.

FLORIS, A., DIÑO, M., JACOBOWITZ, D. M., AND MUGNAINI, E. The unipolar brush cells of the rat cerebellar cortex and cochlear nucleus are calretinin positive: a study by light and electron immunocytochemistry. *Anat. Embryol.* 189: 495–520, 1994.

GEOFFROY, M., LAMBOLEZ, B., AUDINAT, E., HAMON, B., CREPEL, F., ROSSIER, J., AND KADO, R. T. Reduction of desensitization of a glutamatergic ionotropic receptor by antagonists. *Mol. Pharmacol.* 39: 587–591, 1991.

GRASSO, A. AND MERCANTI-CIOTTI, M. T. The secretion of amino acid transmitters from cerebellar primary cultures probed by alpha-latrotoxin. *Neuroscience* 54: 595–604, 1993.

HAMILL, O. P., MARTY, A., NEHER, E., SAKMANN, B., AND SIGWORTH, F. J. Improved patch-clamp techniques for high-resolution current recording from cells and cell-free membrane patches. *Pflügers Arch.* 391: 85–100, 1981.

HARRIS, J., MORENO, S., SHAW, G., AND MUGNAINI, E. Unusual neurofilament composition in cerebellar unipolar brush neurons. *J. Neurocytol.* 22: 663–681, 1993.

HESTRIN, S., SAH, P., AND NICOLL, R. A. Mechanisms generating the time course of dual component excitatory synaptic currents recorded in hippocampal slices. *Neuron* 5: 247–253, 1990.

ISAACSON, J. S. AND NICOLL, R. A. The uptake inhibitor L-*trans*-PDC enhances responses to glutamate but fails to alter the kinetics of excitatory synaptic currents in the hippocampus. *J. Neurophysiol.* 70: 2187–2191, 1993.

ISAACSON, J. S. AND WALMSLEY, B. Counting quanta: direct measurements of transmitter release at a central synapse. *Neuron* 15: 875–884, 1995.

JAARSMA, D., DIÑO, M., COZZARI, C., AND MUGNAINI, E. Cholinergic mossy fibers and their granule cells and unipolar brush cells in rat cerebellar nodulus: a model for central nicotinic neurotransmission. *J. Neurocytol.* 25: 829–842, 1996.

JAARSMA, D., WENTHOLD, R. J., AND MUGNAINI, E. Glutamate receptor subunits at mossy fiber–unipolar brush cell synapses: light and electron microscopic immunocytochemical study in cerebellar cortex of rat and cat. *J. Comp. Neurol.* 357: 145–160, 1995.

JAKAB, R. L. Three-dimensional reconstruction and synaptic architecture of cerebellar glomeruli in the rat. *Acta Morphol. Hung.* 37: 11–20, 1989.

JAKAB, R. L. AND HÁMORI, J. Quantitative morphology and synaptology of cerebellar glomeruli in the rat. *Anat. Embryol.* 179: 81–88, 1988.

JONAS, P. AND SPRUSTON, N. Mechanisms shaping glutamate-mediated excitatory postsynaptic currents in the CNS. *Curr. Opin. Neurobiol.* 4: 366–372, 1994.

JONES, M. V. AND WESTBROOK, G. L. The impact of receptor desensitization on fast synaptic transmission. *Trends Neurosci.* 19: 96–101, 1996.

KINNEY, G. A., OVERSTREET, L. S., AND SLATER, N. T. The slow time course of AMPA receptor-mediated synaptic currents in rat cerebellar unipolar brush cells reflects an entrapment of glutamate in the synaptic cleft. *Soc. Neurosci. Abstr.* 22: 796, 1996.

KINNEY, G. A., ROSSI, D. J., AND SLATER, N. T. Desensitization sculpts the time course of biphasic AMPA receptor-mediated synaptic currents in rat cerebellar unipolar brush cells. *Soc. Neurosci. Abstr.* 21: 586, 1995.

KRIZAJ, D., RICE, M. E., WARDLE, R. A., AND NICHOLSON, C. Water compartmentalization and extracellular tortuosity after osmotic changes in cerebellum of *Trachemys scripta*. *J. Physiol. (Lond.)* 492: 887–896, 1996.

MAKI, R., ROBINSON, M. B., AND DICHTER, M. A. The glutamate uptake inhibitor L-*trans*-pyrrolidine-2,4-dicarboxylate depresses excitatory synaptic transmission via a presynaptic mechanism in cultured hippocampal neurons. *J. Neurosci.* 14: 6754–6762, 1994.

MARGULIS, M. AND TANG, C.-M. The desensitization properties of non-NMDA GluR channels are altered by membrane excision. *Soc. Neurosci. Abstr.* 22: 337, 1996.

MATTOX, D. E., OLMOS, D. R., AND RUBEL, E. W. Freeze-fracture of neurons in nucleus magnocellularis of the chick. *Hear. Res.* 17: 67–78, 1985.

MAYER, M. L. AND WESTBROOK, G. L. The physiology of excitatory amino acids in the vertebrate central nervous system. *Prog. Neurobiol.* 28: 197–276, 1987.

MCBAIN, C. J. AND MAYER, M. L. *N*-methyl-D-aspartic acid receptor structure and function. *Physiol. Rev.* 74: 723–760, 1994.

MENNERICK, S. AND ZORUMSKI, C. F. Presynaptic influence on the time course of fast excitatory synaptic currents in cultured hippocampal cells. *J. Neurosci.* 10: 2385–2399, 1995.

MUGNAINI, E. The histology and cytology of the cerebellar cortex. In: *The Comparative Anatomy and Histology of the Cerebellum. The Human Cerebellum, Cerebellar Connections, and Cerebellar Cortex,* edited by O. Larsell and J. Jansen. Minneapolis, MN: Univ. of Minnesota Press, 1972, p. 201–264.

MUGNAINI, E., DIÑO, M., AND JAARSMA, D. The unipolar brush cells of the mammalian cerebellum and cochlear nucleus: cytology and microcircuitry. *Prog. Brain Res.* 114: 131–149, 1997.

MUGNAINI, E. AND FLORIS, A. The unipolar brush cell: a neglected neuron of the mammalian cerebellar cortex. *J. Comp. Neurol.* 339: 174–180, 1994.

MUGNAINI, E., FLORIS, A., AND WRIGHT-GROSS, M. The extraordinary synapses of the unipolar brush cell: an electron microscopic study in the rat cerebellum. *Synapse* 16: 284–311, 1994.

NAKANISHI, S. Molecular diversity of glutamate receptors and implications for brain function. *Science* 258: 587–603, 1992.

OTIS, T. S., WU, Y.-C., AND TRUSSELL, L. O. Delayed clearance of transmitter and the role of glutamate transporters at synapses with multiple release sites. *J. Neurosci.* 16: 1634–1644, 1996.

PALAY, S. L. AND CHAN-PALAY, V. *Cerebellar Cortex: Cytology and Organization.* New York: Springer-Verlag, 1974.

PARKS, T. N., TAYLOR, D., AND JACKSON, H. Adaptations of synaptic form in an aberrant projection to the avian cochlear nucleus. *J. Neurosci.* 10: 975–984, 1990.

PARTIN, K. M., BOWIE, D., AND MAYER, M. L. Structural determinants of allosteric regulation in alternatively spliced AMPA receptors. *Neuron* 14: 833–843, 1995.

PARTIN, K. M., FLECK, M. W., AND MAYER, M. L. AMPA receptor flip/flop mutants affecting deactivation, desensitization, and modulation by cyclothiazide, aniracetam, and thiocyanate. *J. Neurosci.* 16: 6634–6647, 1996.

PATNEAU, D. K. AND MAYER, M. L. Structure-activity relationships for amino acid transmitter candidates acting at *N*-methyl-D-aspartate and quiqualate receptors. *J. Neurosci.* 10: 2385–2399, 1990.

PATNEAU, D. K., VYKLICKY, L., AND MAYER, M. L. Hippocampal neurons

exhibit cyclothiazide-sensitive rapidly desensitizing responses to kainate. *J. Neurosci.* 13: 3496–3509, 1993.

RAMAN, I. M. AND TRUSSELL, L. O. The kinetics of the response to glutamate and kainate in neurons of the avian cochlear nucleus. *Neuron* 9: 173–186, 1992.

RAMAN, I. M. AND TRUSSELL, L. O. The mechanism of α-amino-3-hydroxy-5-methyl-4-isoxazolepropionate receptor desensitization after removal of glutamate. *Biophys. J.* 68: 137–146, 1995a.

RAMAN, I. M. AND TRUSSELL, L. O. Concentration-jump analysis of voltage-dependent conductances activated by glutamate and kainate in neurons of the avian cochlear nucleus. *Biophys. J.* 69: 1868–1879, 1995b.

ROSENMUND, C., CARR, D. W., BERGESON, S. E., NILAVER, G., SCOTT, J. D., AND WESTBROOK, G. L. Anchoring of protein kinase A is required for modulation of AMPA/kainate receptors on hippocampal neurons. *Nature* 368: 853–856, 1994.

ROSENMUND, C. AND WESTBROOK, G. L. Calcium-induced actin depolymerization reduces NMDA channel activity. *Neuron* 10: 805–814, 1993.

ROSSI, D. J., ALFORD, S., MUGNAINI, E., AND SLATER, N. T. Properties of transmission at a giant glutamatergic synapse in cerebellum: the mossy fiber-unipolar brush cell synapse. *J. Neurophysiol.* 74: 24–42, 1995.

SARANTIS, M., BALLERINI, L., MILLER, B., SILVER, R. A., EDWARDS, M., AND ATTWELL, D. Glutamate uptake from the synaptic cleft does not shape the decay of the non-NMDA component of the synaptic current. *Neuron* 11: 541–549, 1993.

SATHER, W., DIEUDONNE, S,. MACDONALD, J. F., AND ASCHER, P. Activation and desensitization of *N*-methyl-D-aspartate receptors in nucleated outside-out patches from mouse neurones. *J. Physiol. (Lond.)* 450: 643–672, 1992.

SILVER, R. A., TRAYNELIS, S. F., AND CULL-CANDY, S. G. Rapid-time-course miniature and evoked excitatory currents at cerebellar synapses in situ. *Nature* 355: 163–166, 1992.

SLATER, N. T. AND KINNEY, G. A. Reuptake contributes to the removal of glutamate from the synaptic cleft of rat cerebellar granule and unipolar brush cells. *Soc. Neurosci. Abstr.* 22: 796, 1996.

SLATER, N. T., ROSSI, D. J., DIÑO, M., JAARSMA, D., AND MUGNAINI, E. Physiology and ultrastructure of unipolar brush cells of the vestibulocerebellum. In: *Neurochemistry of the Vestibular System,* edited by J. H. Anderson and A. J. Beitz. Boca Raton, FL: CRC, 1997a. In press.

SLATER, N. T., ROSSI, D. J., AND KINNEY, G. A. Physiology of transmission at a giant glutamatergic synapse in cerebellum. *Prog. Brain Res.* 114: 151–163, 1997b.

STORM-MATHISEN, J., DANBOLT, N. C., AND OTTERSEN, O. P. Localization of glutamate and its membrane transport proteins. In: *CNS Neurotransmitters and Neuromodulators: Glutamate,* edited by T. W. Stone. New York: CRC, 1995, p. 1–18,.

TAKAHASHI, M., BILLUPS, B., ROSSI, D., SARANTIS, M., HAMANN, M., AND ATTWELL, D. The role of glutamate transporters in glutamate homeostasis in the brain. *J. Exp. Biol.* 200: 401–409, 1997.

TAKAHASHI, M., KOVALCHUK, Y., AND ATTWELL, D. Pre- and postsynaptic determinants of EPSC waveform at cerebellar climbing fiber and parallel fiber to Purkinje cell synapses. *J. Neurosci.* 15: 5693–5702, 1995.

TANG, C.-M., DICHTER, M., AND MORAD, M. Quisqualate activates a rapidly inactivating high conductance ionic channel in hippocampal neurons. *Science* 243: 1474–1477, 1989.

TRUSSELL, L. O. AND FISCHBACH, G. D. Glutamate receptor desensitization and its role in synaptic transmission. *Neuron* 3: 209–218, 1989.

TRUSSELL, L. O., ZHANG, S., AND RAMAN, I. M. Desensitization of AMPA receptors upon multiquantal neurotransmitter release. *Neuron* 10: 1185–1196, 1993.

VAN KAN, P.L.E., GIBSON, A. R., AND HOUK, J. C. Movement-related inputs to intermediate cerebellum of the monkey. *J. Neurophysiol.* 69: 74–94, 1993.

WRIGHT, D. D., BLACKSTONE, C. D., HUGANIR, R. L., AND RYUGO, D. K. Immunocytochemical localization of the mGluR1α metabotropic glutamate receptor in the dorsal cochlear nucleus. *J. Comp. Neurol.* 364: 729–745, 1996.

WRIGHT, D. D. AND RYUGO, D. K. Mossy fiber projections from the cuneate nucleus to the cochlear nucleus in the rat. *J. Comp. Neurol.* 365: 159–172, 1996.

YAMADA, K. A. AND TANG, C.-M. Benzothiadiazines inhibit rapid glutamate receptor desensitization and enhance glutamatergic synaptic currents. *J. Neurosci.* 13: 3904–3915, 1993.

ZHANG, L., RZIGALINSKI, B. A., ELLIS, E. F., AND SATIN, L. S. Reduction of voltage-dependent Mg^{2+} blockade of NMDA current in mechanically injured neurons. *Science* 274: 1921–1923, 1996.